Supplementary Information for

The VLA-4 integrin is constitutively active in circulating chronic lymphocytic leukemia cells via BCR autonomous signaling: a novel anchor-independent mechanism exploiting soluble blood-borne ligands

Supplementary information:

Supplementary Materials and Methods

IGHV sequence analysis

Sequencing analysis of IGHV was performed on either genomic DNA or complementary DNA using consensus primers for the IGHV leader or the IGHV FR1 regions in conjunction with JH primers, according to LymphoTrack IGHV Leader or IGHV FR1 assays (Invivoscribe), as previously reported [1]. Sequences were analyzed using the IMGT databases and the IMGT/V-QUEST tool (http://imgt.org/, version 3.2.17) [2]. Patients were specifically assigned to the 19 major existing subsets of stereotyped antigen receptor sequences using ARResT/AssignSubset (http://tools.bat.infspire.org/arrest/assignsubsets/) [3].

PBMC and plasma isolation

PBMC were isolated by density-gradient centrifugation (Ficoll-Paque PLUS density gradient media, Cytiva), cryopreserved in 90% fetal bovine serum (FBS, Biowest) plus 10% dimethyl sulfoxide (Sigma-Aldrich), and stored in liquid nitrogen until use. Plasma samples were collected after centrifugation at 2400 g for 10 minutes and stored at -80°C.

VLA-4 activation in whole blood and thawed samples

For the evaluation of constitutive VLA-4 activation, whole blood samples from CLL patients were stained with anti-CD29 PE clone HUTS-21 mAb, anti-CD19 BV421 or PerCpCy5.5 and anti-CD5 PE-Cy7 (all from BD Biosciences) for 20 minutes at room temperature, then lysed with BD FACS™ Lysing Solution and washed with BD® CellWASH (BD Biosciences). Plasma depletion of whole blood through sample washing resulted in significant impairment of HUTS-21 staining (n=38, Supplementary Fig. 1A), confirming the need of plasma for HUTS-21 binding.

Evaluation of bound soluble (s)VCAM-1 was done by labeling whole blood with anti-CD5 FITC (BD Biosciences), anti-CD19 APC (BD Biosciences), anti-HUTS-21 PE and anti-CD106/VCAM-1 PE Vio770 (Miltenyi Biotec). Where indicated, antibody labeling was preceded by lysing and washing blood samples twice.

For staining of thawed PBMC, cells were pre-incubated with an anti-CD49d mAb (clone HP2/1, Sigma-Aldrich) followed by either autologous plasma, recombinant human (rh)VCAM-1 (10µg/ml; R&D) plus 1mM $MnCl_2$ (Sigma-Aldrich) or RetroNectin (10µg/ml; Takara) for 1 hour at 37°C. The cells were then stained with anti-HUTS-21 PE and anti-CD3 APC (BD Biosciences). Addition of

autologous plasma, rhVCAM-1, or RetroNectin to thawed CLL samples, resulted in HUTS-21 binding in CD49d+ CLL (n=17) but not in CD49d- CLL (n=13; Supplementary Fig. 1B). Moreover, pre-incubation of cells with anti-CD49d blocking mAbs (clone HP2/1) before addition of plasma, rhVCAM-1 or RetroNectin, impaired HUTS-21 binding (n=8, Supplementary Fig. 1C).

Cells were acquired on BD FACS CantoII or BD FACS Fortessa X-20 flow cytometers and analysed with FACS DIVA software (BD Biosciences) upon instrument calibration with CS&T beads (BD Biosciences).

ELISA assay

Soluble VCAM-1 was quantified in plasma samples from CLL patients according to the kit instructions, using the human VCAM-1 platinum ELISA (Affimetrix eBioscience).

Phosphoflow on whole blood and thawed samples

Whole blood samples were stained for surface markers (anti-CD3 FITC and anti-HUTS-21 PE or anti-CD3 BUV395, anti-HUTS-21 PE and anti-CD49d BB515). CLL cells were not directly labeled with anti-CD19 and/or -CD5 mAbs to avoid cell stimulation, and were then identified on the basis of negative CD3 expression. In all samples, the amount of non-CLL and non-T cells was negligible. After surface staining for 20 minutes at room temperature, cells were lysed and fixed with BD Phosflow™ Lyse/Fix Buffer (BD Biosciences) for 10 minutes at 37°C. For both whole blood and thawed cell samples (see next section) after the fixation step, the cells were washed with PBS/0.5% BSA, and permeabilized with 70% methanol for 10 minutes on ice. After two washes, cells were stained with one or a combination of the following mAbs for 30 minutes at room temperature: anti-ERK1/2 (pT202/pY204) BV421 or PE, anti-BTK (pY223)/Itk (pY180) BV421 or PE, anti-PLC-γ2 (pY759) Alexa Fluor 647 and anti-AKT (pS473) Alexa Fluor 647 (all from BD Biosciences). After washing, samples were acquired on a LSRFortessa™ X-20 (BD Biosciences).

Soluble VCAM-1 binding assay

PBMC ($1x10^6$ per experimental condition) were thawed, left to recover for 2 hours at 37°C, and where indicated, treated with ibrutinib (1μM) for 1 hour. Cell were then pre-incubated with a blocking anti-CD32 (10μg/ml, BioCell), and where indicated, with a specific VLA-4 integrin antagonist, Firategrast (500nM, MedChemExpress), for 30 minutes at room temperature. Recombinant human (rh)VCAM-1-Fc protein (20μg/ml, R&D), anti-CD3 BUV395 and secondary antibody Alexa Fluor 647-labeled goat anti-human IgG (15ng/μl, Jackson Immunoresearch) were

then added in a $MnCl_2$ containing medium (1mM final concentration). After 20 minutes or 24 hours at 37°C cells were fixed with the BD Phosflow™ Fix Buffer I (BD Biosciences) for 10 minutes at 37°C, before proceeding with the phosphoflow assay.

Actin-polymerization assay by conventional flow cytometry

PBMC ($0.5x10^6$ per experimental condition) were thawed, left to recover for 2 hours at 37°C, then labeled with anti-CD3 APC for 20 minutes, washed and resuspended in RPMI with 1mM $MnCl_2$. Cells were then incubated with or without rhVCAM-1 (10µg/ml) for 1, 2, 3 and 5 minutes at 37°C, immediately fixed, permeabilized and stained by addition of a solution containing 4% formaldehyde, 0.5% Triton X-100 and 0.4U Alexa Fluor 488-conjugated phalloidin (Invitrogen) in PBS for 10 minutes in the dark. Samples were acquired on a LSRFortessa™ X-20 (BD Biosciences). F-actin polymerization was evaluated as the ratio between the phalloidin mean fluorescence intensity (MFI) of VCAM-1 stimulated sample and the control condition.

Actin-polymerization assay by InFlow microscopy

PBMC were thawed, left to recover for 2 hours at 37°C, and pre-incubated with a blocking anti-CD32 (10µg/ml, BioCell) for 30 minutes at room temperature. Cells ($3x10^6$ per experimental condition) were then incubated with rhVCAM-1-Fc (10µg/ml) in a $MnCl_2$ containing medium (1mM final concentration) for 5 minutes at 37°C, then fixed with 4% formaldehyde for 10 minutes, washed, stained with anti-CD3 BV605, anti-CD49d BV421 and secondary antibody Alexa Fluor (AF) 647-labeled goat anti-human IgG, washed and finally permeabilized with 0.5% Triton X-100 and stained with 0.4U AF488-conjugated phalloidin for 30 minutes at room temperature. Single staining controls were prepared in parallel to generate the compensation matrix (see below). Samples (at least 40.000 single CD3- cells) were acquired on an Amnis ImageStreamX Mk II imaging flow cytometer (Cytek Biosciences, CA, USA), X60 magnification with a low flow rate/high sensitivity using INSPIRE software (Cytek Biosciences). For the compensation control, 1000 events for single-stained samples were acquired using the same setting while turning the Ch03 (bright field, BF) and 785 nm laser (side scatter, SSC) off. Ideas software (IDEAS 6.2.187.0, Cytek Biosciences) was used for compensation analysis and for data analysis. The channels were as follows: Ch1: CD49d BV421; Ch2: phalloidin-AF488; Ch3: BF; Ch4: CD3 BV605; Ch5: VCAM-1 AF647; Ch6: SSC. For the analyses the following gating strategy was used: Gradient RMS based on Ch3 (BF) was used to select focused cells; Area and Aspect Ratio on Ch3 were used to select single cells, and Area on Ch3 versus Intensity of Ch6 (SSC) defined homogeneous lymphocytes; CD3+ cells were excluded by plotting Area Ch3 and Intensity of Ch4 (CD3); CD49d+ phalloidin+ cells

were selected on a Intensity Ch1 versus Intensity Ch2 plot; VCAM-1 bound and VCAM-1 not bound cells were gated on the basis of Intensity of Ch5 (Supplementary Fig. 5). Each region was validated by visual inspection of the image Gallery. A region of interest (called mask) covering all pixels containing a fluorescence signal is automatically established for each cell, for each channel. Within the mask in Ch2, the fluorescence intensity of F-actin staining was calculated as intensity (sum of the intensities of each pixel in the mask). The circularity feature, used to quantify actin polarization is a mathematical expression equation of the IDEAS software. It calculates the ratio between the average distance from the mask center to the boundaries and the variation of the distance. The more a mask deviates from a circle the lower is the circularity result.

TKO cell lines

TKO cells are bone-marrow-derived cells from mice deficient for Rag2, λ5, and SLP-65 (triple-knock-out) and express 4-hydroxy-tamoxifen (4-OHT) inducible fusion protein ER^{T2}-SLP65. TKO cells are retroviral-transduced to express CLL derived BCR [4, 5]. Transduction efficiencies were monitored by FACS analyses for IgM expressing cells after 2, 4 and 6 days and computed for the competitive proliferation of BCR positive cells compared to untransduced, BCR negative cells. Positively transduced cells were FACS sorted by surface IgM labeling with fluorescence-coupled anti-IgM Fab fragment antibody to avoid aberrant BCR stimulation before analyses. Sorted BCR expressing cells were maintained in culture and analyzed for autonomous signaling/antigen-induced signaling by Ca^{2+} influx read-out. The list of the generated TKO cell lines is summarized in Supplementary Table 3.

TKO cells were cultured in Iscove's medium (Sigma-Aldrich) containing 2mM L-glutamine (Life Technology), 5% heat-inactivated fetal bovine serum (FBS, Biowest) and 100U/ml of penicillin/streptomycin (Gibco), 50mM β-mercaptoethanol (Sigma-Aldrich) and 1ng/ml murine IL-7 (Immunotools). For inhibition experiments, ibrutinib (5μM; MedChemExpress), Idelalisib (5μM; MedChemExpress), a combination of ibrutinib and idelalisib, companlisib (5μM; MedChemExpress) or vehicle alone from a 5mM stock in DMSO was added to TKO cells 1 hours before the assay.

Real-time kinetic VLA-4 affinity assay on TKO cells and primary CLL cells

VLA-4 affinity was cytometrically analyzed in TKO cells ($1x10^6$per experimental condition) at 37°C under agitation using the FACSAriaIII flow cytometer. Upon establishing an autofluorescence baseline for 60s, 4nM fluorochrome-conjugated tri-peptide (LDV-FITC; TOCRIS) was added and

data were acquired for further 60s before PBS, 4-hydroxy-tamoxifen (4-OHT, 2μM; MedchemExpress), 4-OHT plus $F(ab)_2$ anti-IgM (10μg/ml; Jackson Immunoresearch) or manganese (Mn^{2+}, 3mM; Sigma-Aldrich) was added. Upon further 240s, samples were treated with 500-fold excess of unlabeled LDV probe (2μM; TOCRIS), and the dissociation of LDV-FITC was followed for further 180s. The same scheme was followed for VLA-4 affinity in CLL samples, using in sequence LDV-FITC, PBS and unlabeled LDV. The resulting data were converted to MFI of the FITC channel versus time using R software (http://www.r-project.org) and analysed by GraphPad Prism5. To obtain the dissociation rate constants (K_{off}), the data were fitted to a one-phase exponential decay equation: $K_{off}<0.02s^{-1}$ high affinity, $K_{off}>0.06s^{-1}$ low affinity.[6]

VLA-4 activation assay on CLL cells

Thawed PBMC ($2x10^5$ per experimental condition) were incubated with a range of concentrations of the VLA-4 specific ligand, LDV in the presence of an excess of anti-HUTS-21 PE, for 30 min at 37°C, as reported [7, 8]. A mixture of anti-CD3 FITC (BD Biosciences), anti-CD19 APC and DAPI (Sigma-Aldrich) were added during the last fifteen minutes incubation. Subsequently, the MFI of labeled HUTS-21 mAb was measured, and VLA-4 receptor occupancy (RO) was determined ranging from 0.0 (no RO) to 1.0 (100% RO), as reported [7, 8]. RO was also used as an indicator of binding affinity (at 10nM LDV), where higher RO indicates larger fraction of high affinity receptors [7].

Calcium assay

TKO cells ($1x10^6$per experimental condition) were incubated in Iscove's basal medium (Sigma-Aldrich) 1% FBS with 1μM Indo-1 AM (BD Biosciences) for 30 minutes at 37°C. Cells were then washed, resuspended in RPMI with 1% FBS at $5x10^6$ cells/ml and acquired at 37°C on FACSAriaIII (BD Biosciences). After a baseline acquisition for 60s, cells were stimulated with 4-OHT (2μM, MedchemExpress), 4-OHT plus $F(ab)_2$ anti-IgM (anti-IgM, 10μg/ml; Jackson Immunoresearch) or calcimycin (1μg/ml Thermofisher) and recorded for another 6 minutes.
To calculate the percentage of cells that exhibited increased fluorescence following stimuli (% responding cells) a background fluorescence threshold (T) at the fluorescence intensity of the 85^{th} percentile of unstimulated cells was established for each sample, and then the peak percentage of cells that exhibited an increase in fluorescence intensity above T following treatment with 4-OHT or 4-OHT plus anti-IgM was calculated [9]. Data were analysed by FlowJo software (Version 10, TreeStar).

References

1. Leich E, Maier C, Bomben R, Vit F, Bosi A, Horn H, et al. Follicular lymphoma subgroups with and without t(14;18) differ in their N-glycosylation pattern and IGHV usage. Blood Adv. 2021;5:4890-4900.
2. Brochet X, Lefranc MP, Giudicelli V. IMGT/V-QUEST: the highly customized and integrated system for IG and TR standardized V-J and V-D-J sequence analysis. Nucleic acids research. 2008;36:W503-508.
3. Bystry V, Agathangelidis A, Bikos V, Sutton LA, Baliakas P, Hadzidimitriou A, et al. ARResT/AssignSubsets: a novel application for robust subclassification of chronic lymphocytic leukemia based on B cell receptor IG stereotypy. Bioinformatics. 2015;31:3844-3846.
4. Köhler F, Hug E, Eschbach C, Meixlsperger S, Hobeika E, Kofer J, et al. Autoreactive B Cell Receptors Mimic Autonomous Pre-B Cell Receptor Signaling and Induce Proliferation of Early B Cells. Immunity. 2008;29:912-921.
5. Meixlsperger S, Köhler F, Wossning T, Reppel M, Müschen M, Jumaa H. Conventional light chains inhibit the autonomous signaling capacity of the B cell receptor. Immunity. 2007;26:323-333.
6. Chigaev A, Blenc AM, Braaten JV, Kumaraswamy N, Kepley CL, Andrews RP, et al. Real time analysis of the affinity regulation of alpha 4-integrin. The physiologically activated receptor is intermediate in affinity between resting and Mn(2+) or antibody activation. J Biol Chem. 2001;276:48670-48678.
7. Chigaev A, Waller A, Amit O, Halip L, Bologa CG, Sklar LA. Real-time analysis of conformation-sensitive antibody binding provides new insights into integrin conformational regulation. JBiolChem. 2009;284:14337-14346.
8. Tissino E, Benedetti D, Herman SEM, Ten Hacken E, Ahn IE, Chaffee KG, et al. Functional and clinical relevance of VLA-4 (CD49d/CD29) in ibrutinib-treated chronic lymphocytic leukemia. J Exp Med. 2018;215:681-697.
9. Mockridge CI, Potter KN, Wheatley I, Neville LA, Packham G, Stevenson FK. Reversible anergy of sIgM-mediated signaling in the two subsets of CLL defined by VH-gene mutational status. Blood. 2007;109:4424-4431.

Supplementary Tables

Supplementary Table 1. Clinical and biological features of 1034 CD49d positive CLL cases.

Factor	Data available, n	Cases, n (%)
age, median (range), years[a]	1032	69 (32-92)
<65		376 (36.4)
≥65		656 (63.6)
Gender	1034	
male		649 (62.8)
female		385 (37.2)
Rai stage	369	
0		125 (33.9)
I		131 (35.5)
II		72 (19.5)
III		18 (4.9)
IV		23 (6.2)
FISH category[b]	836	
del17p		121 (14.5)
del11q		90 (10.8)
tri12		243 (29.0)
del13q		188 (22.5)
normal		194 (23.2)
IGHV mutational status	911	
unmutated		510 (56.0)
mutated		364 (40.0)
multiple rearrangement		37 (4.0)
TP53 mutational status[c]	827	
mutated		189 (22.9)
wild type		638 (77.1)
NOTCH1 mutational status	657	
mutated		458 (69.7)
wild type		199 (30.3)

[a]age at sampling; [b]according to Döhner et al (N Engl J Med. 2000;343:1910-6); [c]TP53 mutated cases included cases with low VAF TP53 mutation, as reported (Clin Cancer Res 2021;27:5566-75)

Supplementary Table 2. BCR features of 874 CLL cases with a single productive rearrangement.

		n (%)
IGHV families (n=874)	V_H 1	254 (29.1)
	V_H 2	23 (2.6)
	V_H 3	374 (42.8)
	V_H 4	181 (20.7)
	V_H 5	30 (3.4)
	V_H 6	7 (0.8)
	V_H 7	5 (0.6)
BCR stereotypic subsets (n=118)	#1	38 (32.2)
	#2	18 (15.3)
	#3	3 (2.5)
	#4	1 (0.8)
	#5	7 (5.9)
	#6	11 (9.3)
	#7H	2 (1.7)
	#8	8 (6.8)
	#14	3 (0.3)
	#28A	7 (5.9)
	#59	4 (0.5)
	#64B	2 (5.9)
	#77	1 (0.8)
	#99	9 (1)
	#201	3 (0.3)
	#202	1 (0.8)

Supplementary Table 3. List of TKO cell lines.

Cell line group	Patients code	IGHV	IGHD	IGHJ	% homology	HCDR3 Sequence	Subset	Light Chain	IGLV	IGLJ	LCDR3
TKO-high	UD4	IGHV3-21*01		IGHJ6*02	95.8	ARDQNGMDV	2	Lambda	IGVL3-21	IGLJ3-02	QVWDSSSDHPWV
	RMPTV327	IGHV3-21*01	IGHD2-15*01	IGHJ6*02	97.9	ARDRSGMDV	2	Lambda	IGVL3-21	IGLJ3-02	QVWDSSSDHPWV
	CT292	IGHV4-34*01	IGHD6-19*01	IGHJ3*02	90.2	ARDIEVALPDAFDI		Kappa	IGVK3-11	IGKJ2-01	QQRNWPLYT
	UD134	IGHV3-21*01	IGHD3-10*01	IGHJ3*02	95.5	ARHRGYGSGTNDAFDI		Kappa	IGVK1D-8	IGKJ2-02	QQYYTFPARL
TKO-low	TS312	IGHV1-2*02	IGHD6-19*01	IGHJ4*02	100.0	AREQWLVSPHFDY	1	Kappa	IGVK1-39	IGKJ1-01	QQSYSTPPWT
	RIO128	IGHV1-2*02	IGHD3-10*01	IGHJ6*02	100.0	ARDRIPGLMVRGVPPTGYGMDV		Lambda	IGVL3-1	IGLJ1-01	QAWDSSTAHYV
	RM833	IGHV1-2*02	IGHD1-26*01	IGHJ4*02	100.0	ARDPLVYSGSYGTLLDY		Lambda	IGVL1-40	IGLJ2-01	QSYDSSLSPVV
	RMPTV332	IGHV1-2*02	IGHD6-19*01	IGHJ4*02	100.0	ARVQWWLVPGFDY	1	Kappa	IGVK1-39	IGLJ3-01	QQSYSTPPFTF
TKO-mod	CT292 mod	IGHV4-34*01	IGHD6-19*01	IGHJ3*02	90.2	ARDIEVALPDAFDI		Kappa	IGVK1-39	IGLJ3-01	QQSYSTPPFT
	UD134 mod	IGHV3-21*01	IGHD3-10*01	IGHJ3*02	95.5	ARHRGYGSGTNDAFDI		Kappa	IGVK1-39	IGLJ3-01	QQSYSTPPFT
	UD134 mod	IGHV3-21*01	IGHD3-10*01	IGHJ3*02	95.5	ARHRGYGSGTNDAFDI		Kappa	IGVK3-15	IGLJ1-01	QQYNNWPRGT

Supplementary Figures (with legends)

Supplementary Fig. 1

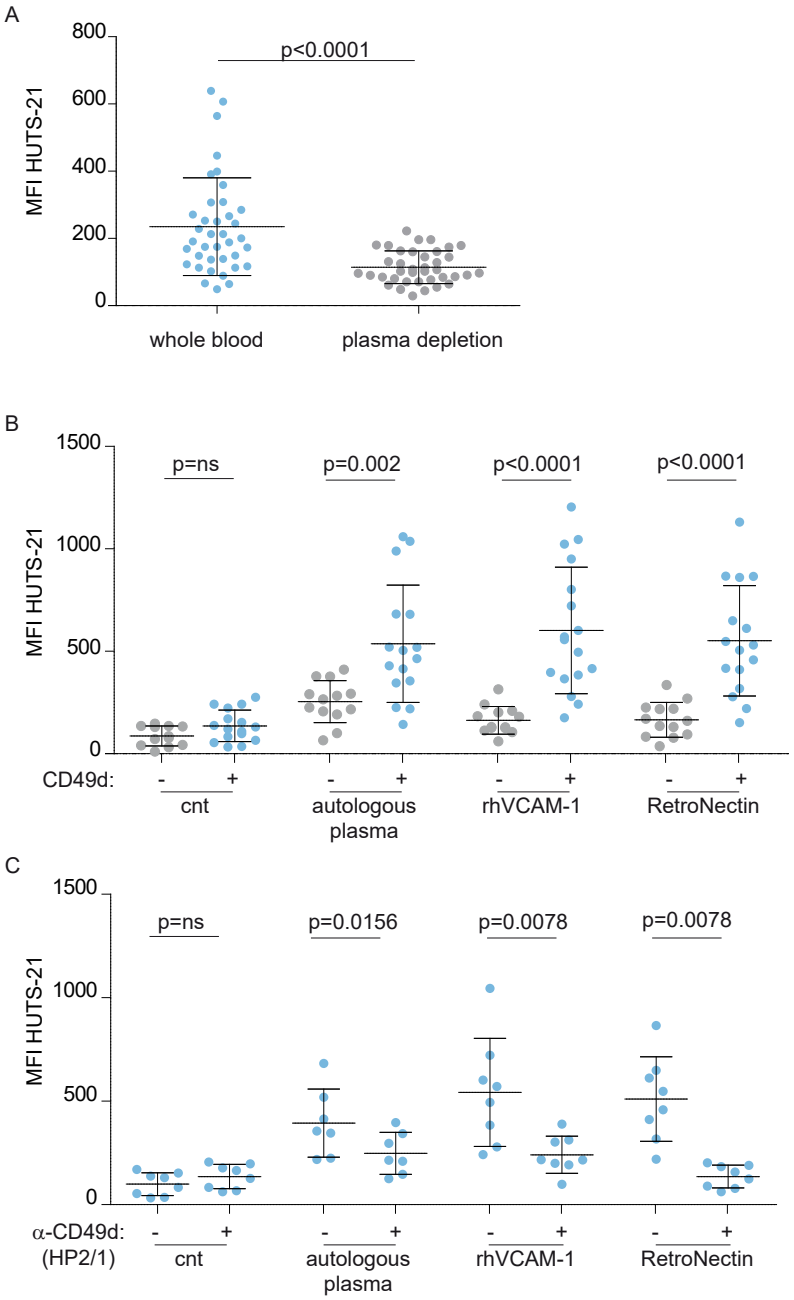

Supplementary Fig. 1: Validation of HUTS-21 staining. (A) Fresh whole blood samples (blue dots) or whole blood samples after plasma depletion (grey dots) from 38 CD49d+ CLL cases were stained with HUTS-21 mAb and analysed by flow cytometry. Levels of HUTS-21 binding are reported as MFI values analysed on CD19+CD5+ cells. (B) Binding of HUTS-21 mAbs was evaluated in thawed cells from CD49d- (grey dots; n=13) and CD49d+ (blue dots; n=17) CLL cases, at the following conditions: control (cnt), after the addition of autologous plasma, recombinant human (rh)VCAM-1 and RetroNectin. (C) Levels of HUTS-21 binding was evaluated in thawed cells from CD49d+ CLL cases (n=8) pre-incubated or not with the anti-CD49d HP2/1 blocking mAb (α-CD49d) before addition of autologous plasma, rhVCAM-1 or RetroNectin. Data are presented as mean ± SD MFI. P-values refer to Mann-Whitney (B) and Wilcoxon (A-C) test; ns, not significant.

Supplementary Fig. 2

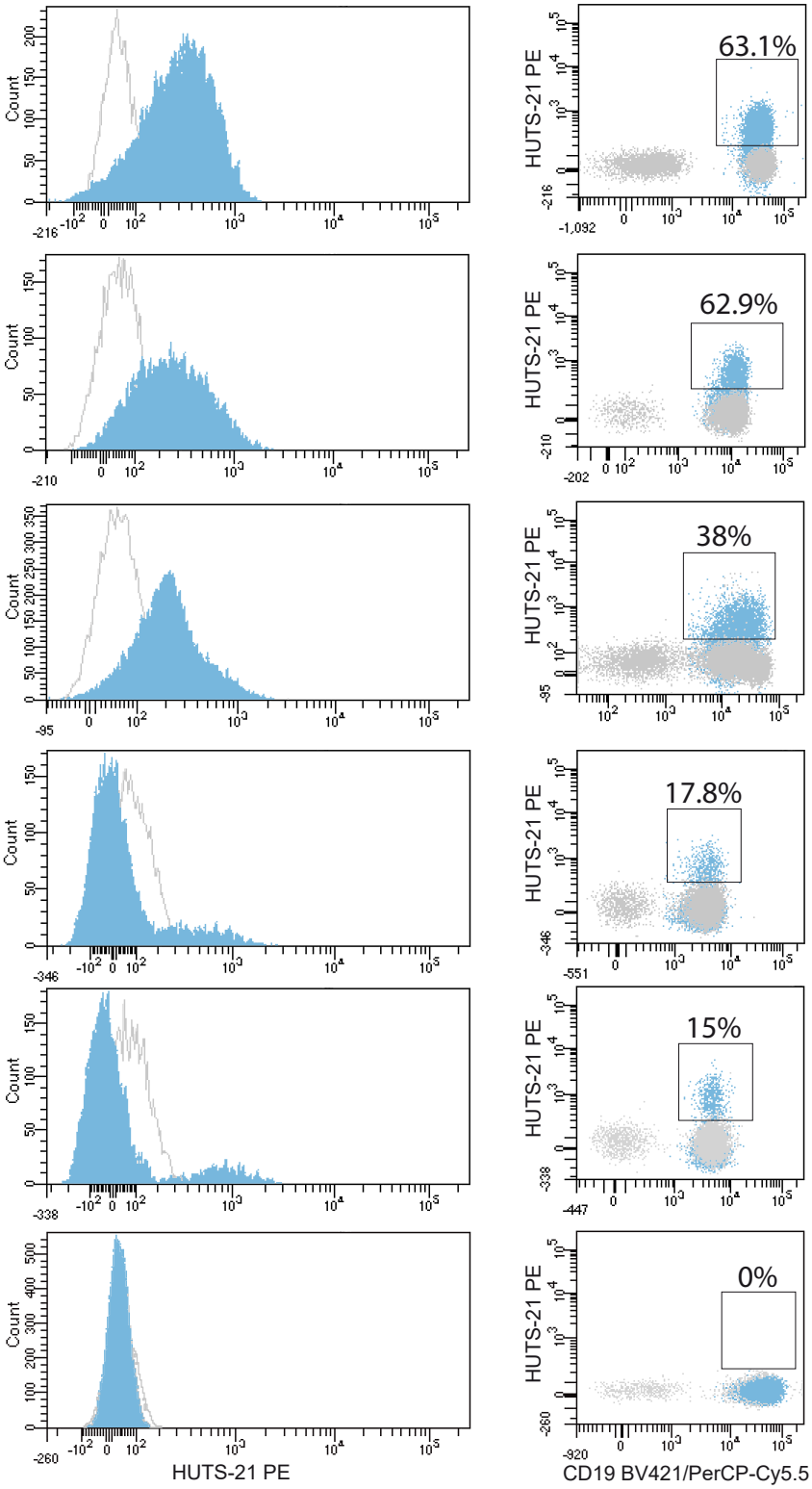

Supplementary Fig. 2: HUTS-21 staining in CLL whole blood. The histogram plots show different levels and pattern of HUTS-21 binding as representative of the entire case cohort; the levels of HUTS-21 binding, evaluated as percentage of positive CLL cells are shown to the right of each histogram. The grey histogram refers to unstained control.

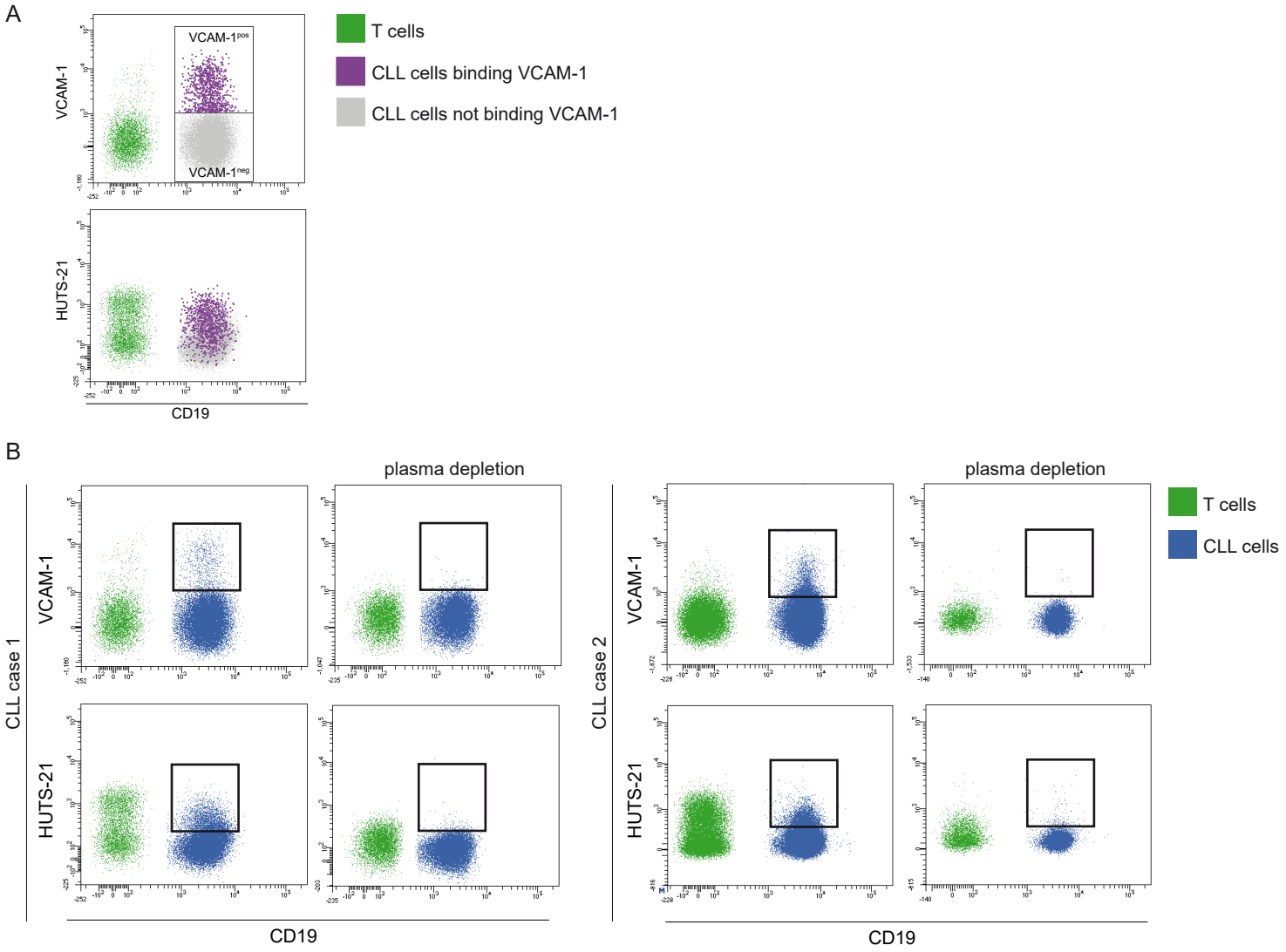

Supplementary Fig. 3: Specificity of VCAM-1 staining. (A) Gating strategy used for the analysis of HUTS-21 in circulating CLL cells bound or not to sVCAM-1 in a representative CLL case; CD19+ CLL cells (concomitantly expressing CD5, not shown) were split in VCAM-1^{pos} (purple) and VCAM-1^{neg} (grey) according to VCAM-1 binding levels above or below the threshold set on the unstained control (upper plot); CD19 versus HUTS-21 in the previously gated populations (lower plot); the green dots (CD19-) correspond to T cells. (B) Dot plots of VCAM-1 (above) and HUTS-21 (below) vs CD19 staining in whole blood (left and middle right plots) or in plasma depleted (middle left and right plots) samples from two representative CLL cases. Blue and green dots refer to CLL and T cells respectively.

Supplementary Fig. 4

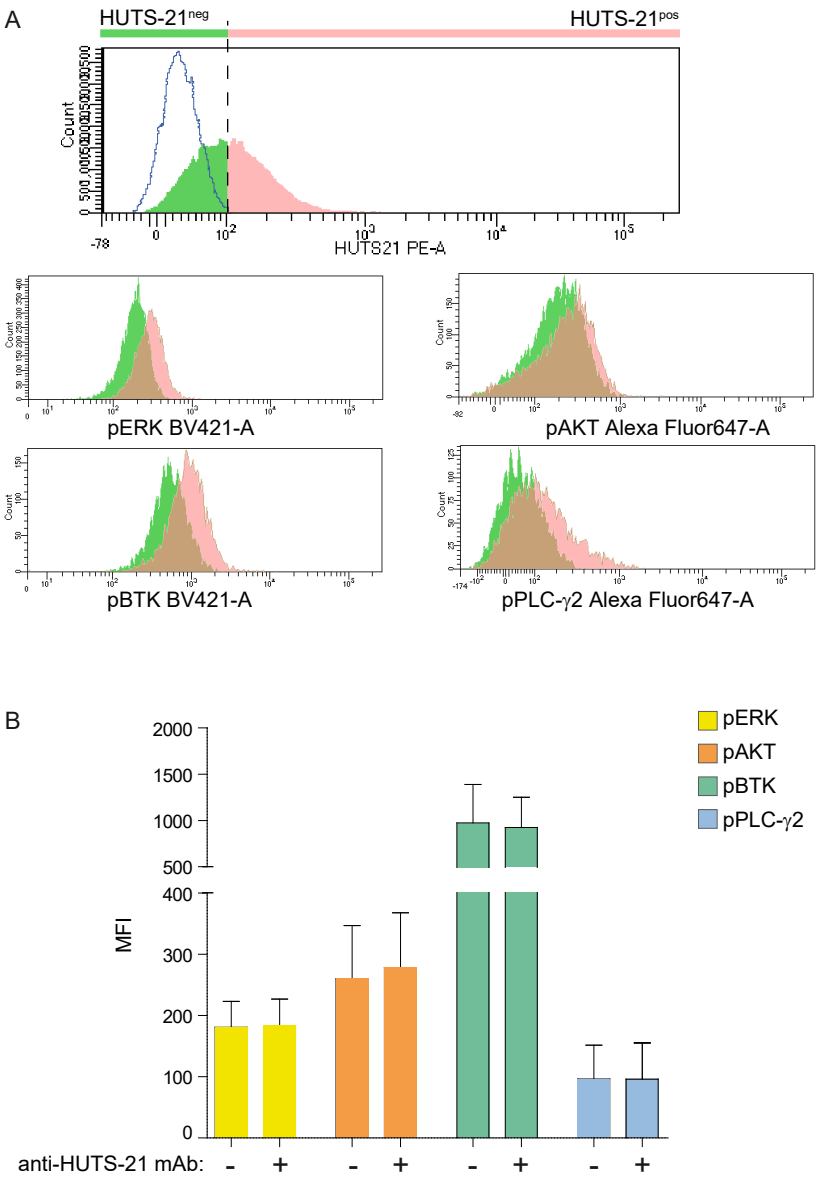

Supplementary Fig. 4: Phosphorylation levels of signalling proteins according to HUTS-21 binding levels. (A) Histogram plots show expression for each phospho-proteins in HUTS-21^{neg} (green histogram) and HUTS-21^{pos} (pink histogram) cells from a representative CLL sample. (B) Phosphorylation levels of ERK1/2, AKT, BTK and PLC-γ2 in whole blood samples previously labelled or not with anti-HUTS-21 mAb. Phosphoprotein expression, reported as MFI values, was analysed in the context of CD3- cells.

Supplementary Fig. 5

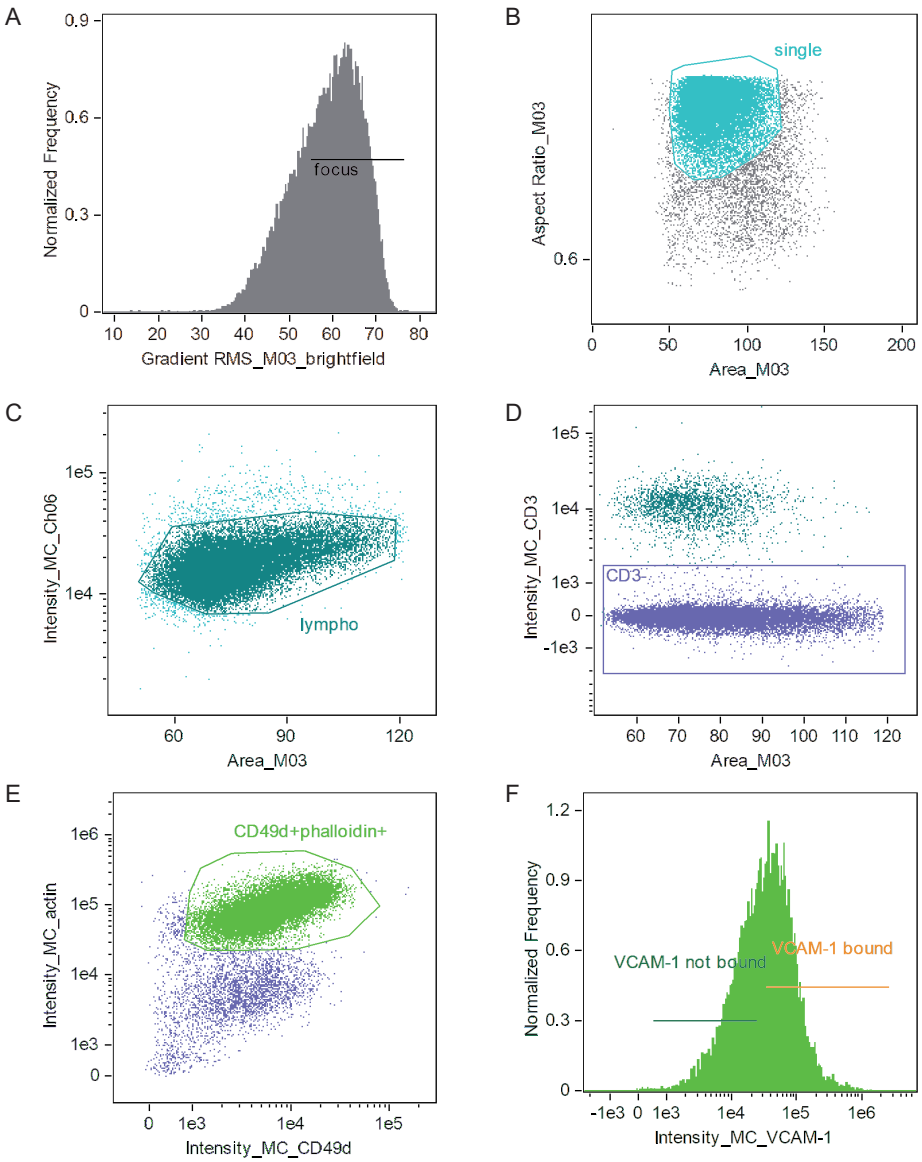

Supplementary Fig. 5: Gating strategy for InFlow microscopy analyses. Images were analysed with IDEAS software. The channels were as follows: Ch1: CD49d BV421; Ch2: phalloidin-AF488; Ch3: bright field (BF); Ch4: CD3 BV605; Ch5: VCAM-1 AF647; Ch6: side scatter (SSC). (A) Focused cells were selected using Gradient RMS feature based on Ch3 (BF); (B) Area and Aspect Ratio on Ch3 were used to select single cells; (C) Area on Ch3 versus Intensity of Ch6 (SSC) defined homogeneous lymphocytes; (D) CD3- cells were gated on an Area Ch3 versus Intensity of Ch4 (CD3) plot; (E) CD49d+ phalloidin+ cells were selected on a Intensity Ch1 versus Intensity Ch2 plot; (F) VCAM-1 bound and VCAM-1 not bound cells were gated on the basis of Intensity of Ch5. Each region was validated by visual inspection of the image Gallery.

Supplementary Fig. 6

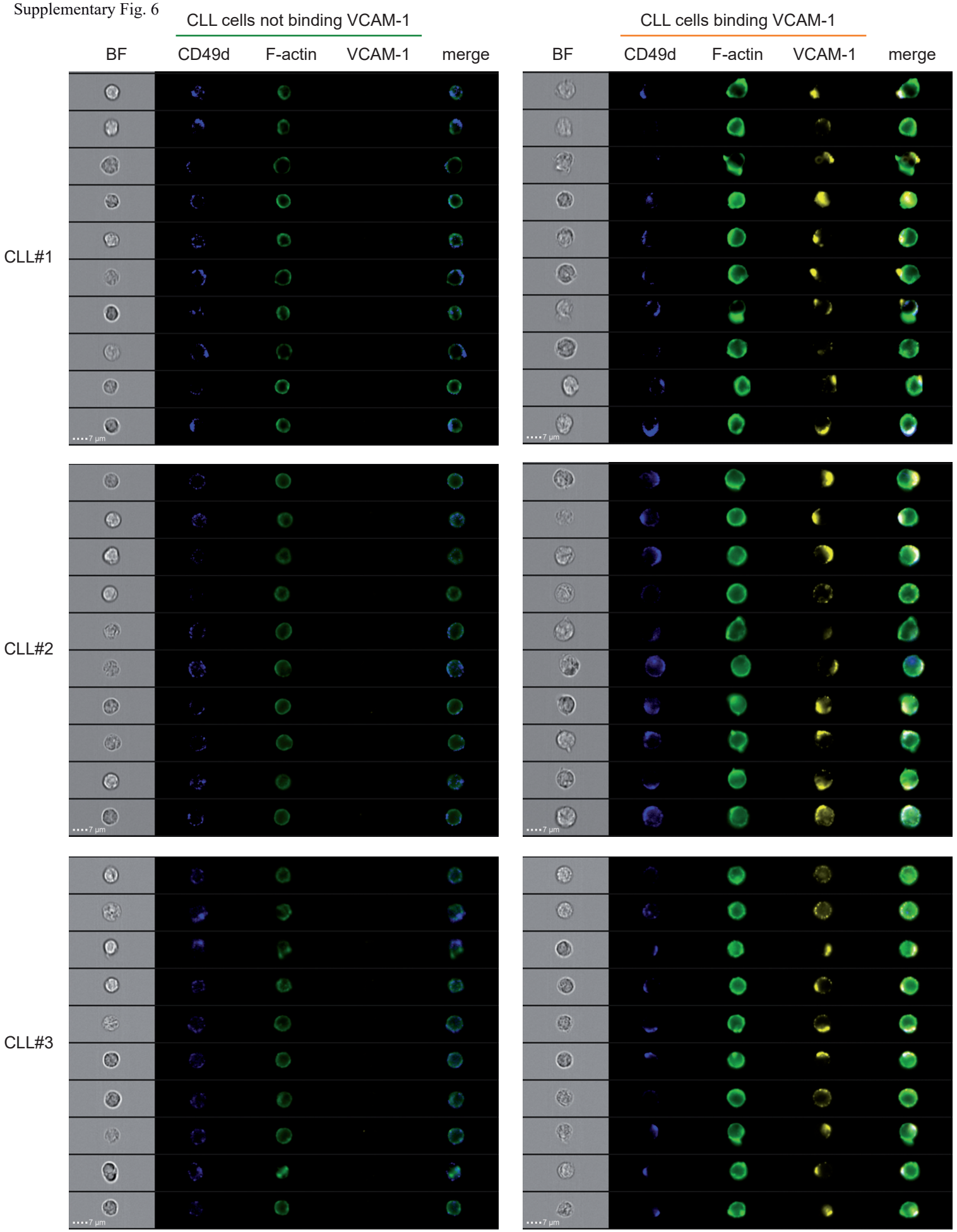

Supplementary Figure 6: InFlow microscopy sample images. Images from cells not binding VCAM-1 (left) and cells binding VCAM-1 (right), according to the gating shown in Supplementary Figure 5, in three different CLL samples. The displayed gallery columns are, from left to right: bright field (BF, grey), CD49d (blue), F-actin (green), VCAM-1 (yellow) and the merging of CD49d/F-actin/VCAM-1. Image display pixel intensity range for all the channels was set and fixed in the cells binding VCAM-1 condition for each sample, and is therefore equal between the left and right images.

Supplementary Fig. 7

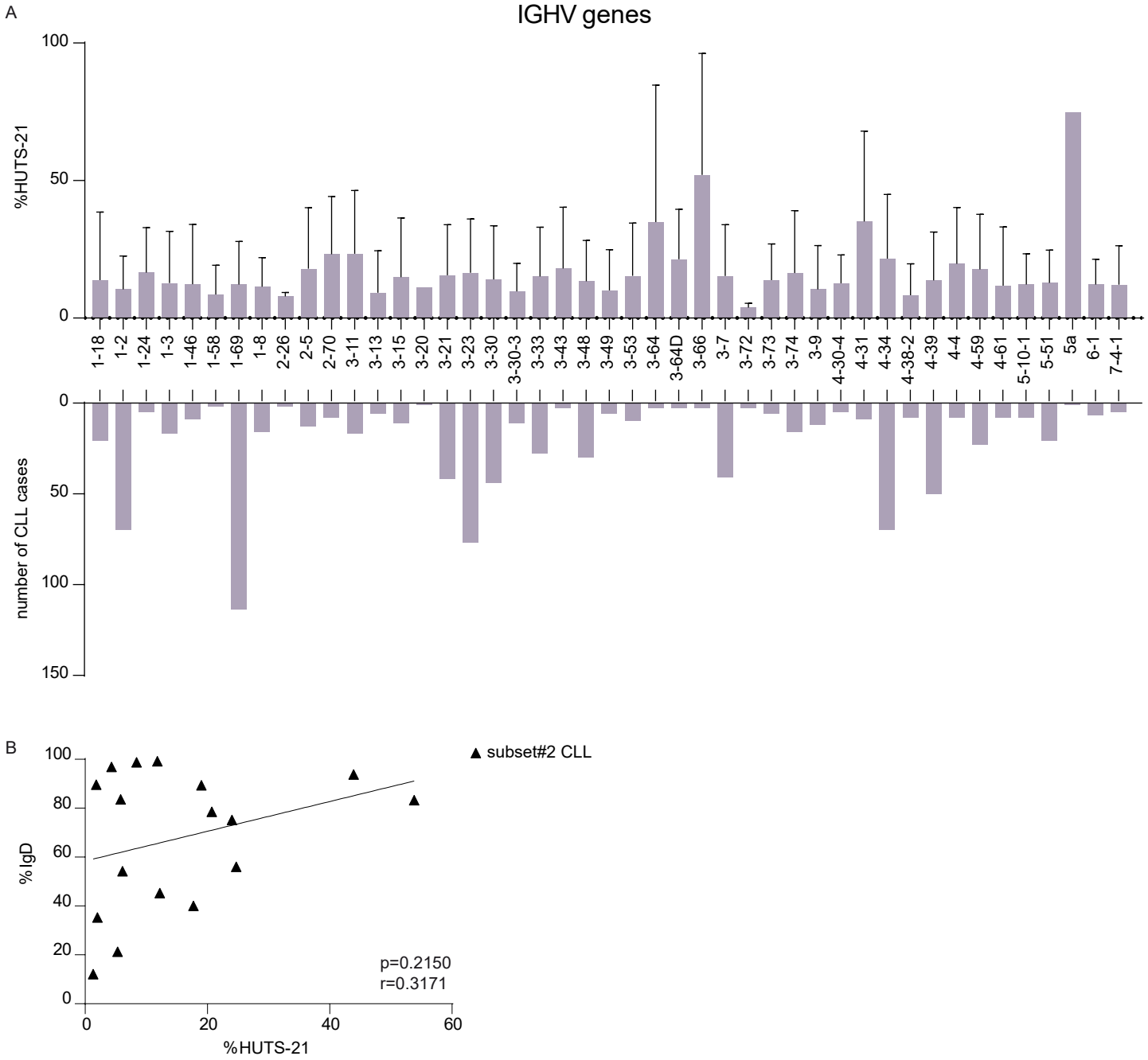

Supplementary Fig. 7: VLA-4 activation in CLL split according to IGHV gene usage and correlation between IgM and IGD expression in the context of subset#2 and #1. (A) Levels of HUTS-21 binding evaluated as percent of positive cells in CLL cases split according to the IGHV gene usage (upper bar chart) and number of cases for each IGHV gene (lower bar chart). (B) In the context of CLL from subset#2, the levels of HUTS-21 binding evaluated as percent of positive cells was correlated to IgD expression (%). The correlation coefficient (r) and p-value were obtained by the Pearson's method.

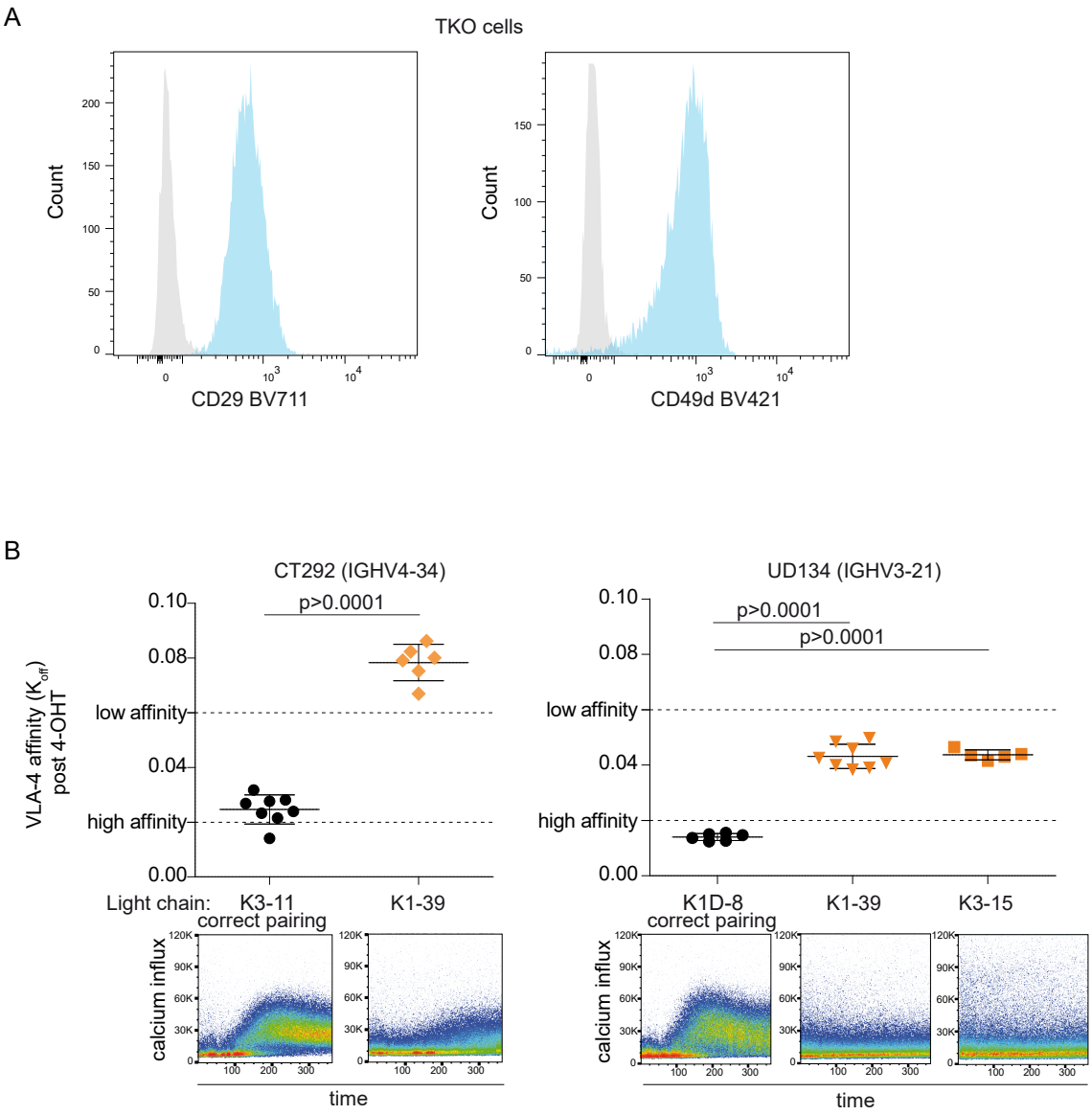

Supplementary Fig. 8: VLA-4 expression by triple-knockout (TKO) cells and effect of Ig heavy and light chain combinations on BCR autonomous signaling and VLA-4 affinity. (A) Expression of the VLA-4 integrin subunits CD29 (left) and CD49d (right) was evaluated by flow cytometry in TKO cells. The reported histogram plots are representative of all TKO cells with different CLL-derived BCRs analysed. (B) Comparison of VLA-4 affinity state of TKO cells expressing either the actual CLL-derived Ig light chain (correct pairing, black symbols) or a different Ig light chain (orange symbols). The pseudocolored dot plots show the corresponding calcium influx over time (in seconds) for each TKO cell line stimulated by 4-OHT. Individual symbols represent an experimental replication for each tested TKO cell line. P-values refer to the unpaired t test.